Journal of Coastal Research	14	3	1099–1108	Royal Palm Beach, Florida	Summer 1998

Laboratory and Field Observations of the Joint Distribution of Shoaling Wave Heights and Periods

J.C. Doering

Hydraulics Research & Testing Facility
Civil and Geological Engineering
University of Manitoba
Winnipeg, Manitoba
Canada R3T 5V6

ABSTRACT

DOERING, J.C., 1998. Laboratory and field observations of the joint distribution of shoaling wave heights and periods. *Journal of Coastal Research*, 14(3), 1099–1108. Royal Palm Beach (Florida), ISSN 0749-0208.

The evolution of the joint distribution of wave heights and periods that arises during shoaling is investigated using laboratory and field data. The laboratory data were obtained from experiments conducted on a 1:20 planar beach slope, while the field data were obtained from a nearly planar beach with a nearshore slope of approximately 1:25. The data are compared to the theoretical distribution proposed by Longuet-Higgins. Both the laboratory and field data indicate that for unbroken waves with $\nu \lesssim 0.35$ the shapes of the observed and predicted distributions are in relatively good agreement.

ADDITIONAL INDEX WORDS: *Joint distribution, shoaling waves.*

INTRODUCTION

The joint distribution of wave heights and periods is of interest to coastal scientists and engineers. It can be used to derive other joint distributions (*e.g.*, heights and slopes) or marginal distributions (*e.g.*, wave steepness). The engineering importance of the joint distribution of wave heights and periods is not at all surprising, as it is well-known that wave-induced forces arise from pressure, velocities, and accelerations, all of which are a function of both wave amplitude (height) and period.

The first approximation for the joint distribution of wave heights and periods was proposed by WOODING (1955), who extended the work of RICE (1944, 1945). LONGUET-HIGGINS (1957) independently proposed a similar formulation for the joint distribution of wave heights and periods. LONGUET-HIGGINS (1983) later modified his work to account for the asymmetry observed (*e.g.*, GODA, 1978) in the distribution of wave periods.

CAVANIÉ *et al.* (1976) developed a model for the joint distribution of wave heights and periods starting from the work of CARTWRIGHT and LONGUET-HIGGINS (1956), at about the same time as LONGUET-HIGGINS (1975). The distribution proposed by CAVANIÉ *et al.* (1976) accounts for the asymmetry observed in the wave period distribution.

The models of LONGUET-HIGGINS (1983) and CAVANIÉ *et al.* (1976) are expressed in a closed analytical form that depends only on a (different) spectral width parameter. The spectral width parameter ϵ, defined by CAVANIÉ *et al.* (1976) involves fourth-order moments of the variance density spectrum, making it extremely sensitive to the high frequency cut-off (SROKOSZ and CHALLENOR, 1987). For a typical wave spectrum this means that the estimate of ϵ will not converge as the high frequency tail typically falls off as f^{-4}. This shortcoming makes the joint distribution of CAVANIÉ *et al.* (1976) impractical to use. On the other hand, the spectral width pa-

97021 received 24 February 1997; accepted in revision 5 September 1997.

Table 1. *Summary of data.*

Environment	Run ID	T_p [sec]	H_s[1] [m]
Laboratory	GR18-21	1.67	0.14
	GR22-25	1.67	0.25
Field	QA25G4-I1	6.3	0.81
	QA29N5-P2	8.0	0.40

[1]The estimate of H_s, the characteristic wave height, is at the deepest sensor

Table 2. *Summary of parameters for data.*

Run	Sensor	d [m]	ν
GR18-21	WP 1	0.944	0.30
	WP 7	0.357	0.35
	WP 9	0.162	0.42
GR22-25	WP 1	0.944	0.25
	WP 7	0.357	0.37
	WP 9	0.162	0.42
QA25N5-P2	P2	4.29	0.34
	P4	3.19	0.38
	P6	0.97	0.43
QA29G4-I1	P2	4.59	0.35
	P4	3.31	0.37
	P6	1.24	0.41

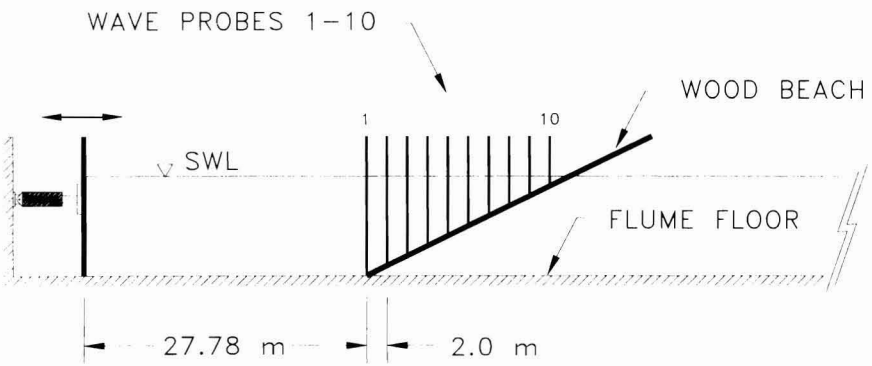

Figure 1. Cross-section of 1:10 scale experimental arrangement used for 1:20 beach slope.

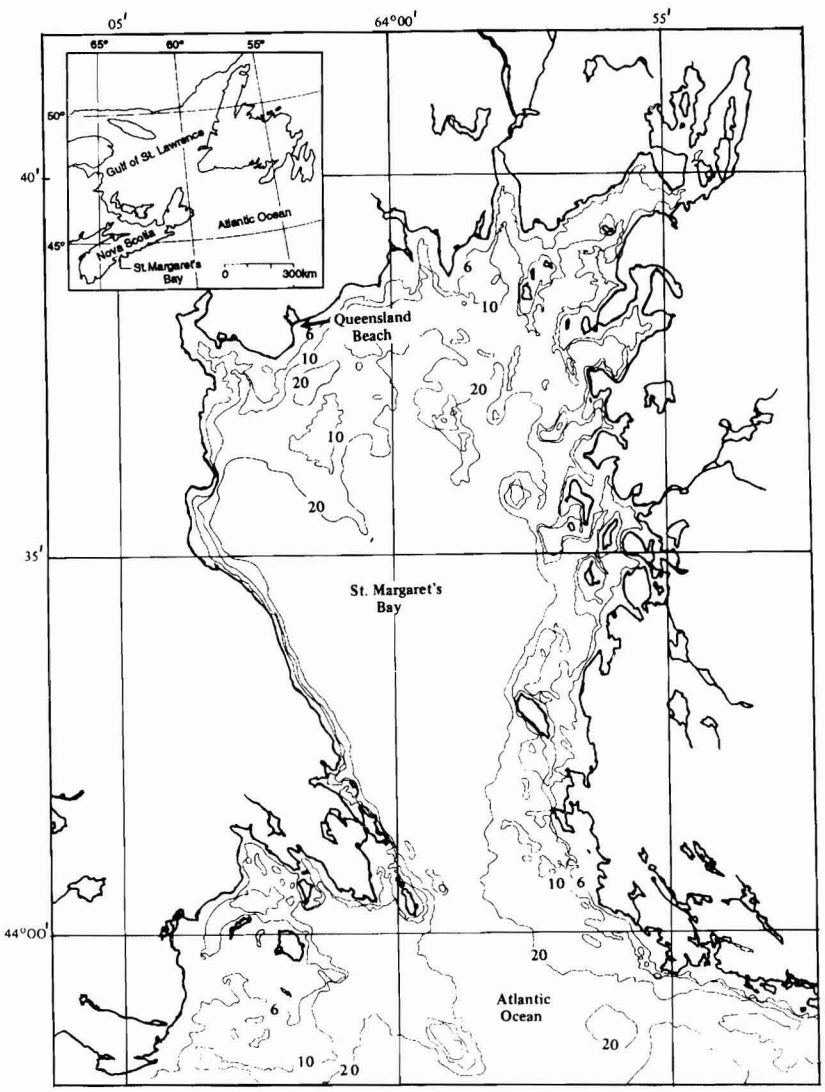

Figure 2. Field site, Queensland Beach, St. Margaret's Bay, Nova Scotia, Canada (from Osborne and Greenwood, 1992). Note: contours are in fathoms.

rameter ν, defined by Longuet-Higgins (1983) depends on only the lowest three moments of the variance density spectrum. LONGUET-HIGGINS (1983) assumes his distribution is applicable to a narrow spectrum of waves, *i.e.*, $\nu^2 \ll 1$. LONGUET-HIGGINS (1983) assumes this condition is satisfied when $\nu \leq 0.6$. For a fully-developed spectrum of deep-water waves (*i.e.*, f^{-4}) this yields a value for ν of ≈ 0.3, which is well below the "upper limit" of 0.6.

LINDGREN and RYCHLIK (1982) and YUAN (1982) have also proposed models to predict the joint distribution of wave heights and periods. Like the model proposed by CAVANIÉ *et al.* (1976), these models depend on fourth-order moments of the wave spectrum and are as a result quite sensitive to the high frequency cut-off.

The bulk of previous research on the joint distribution of wave heights and periods has focused on deep water waves. As a result, the applicability of various models to shoaling and shallow water waves has not been widely explored. Yet this information is of practical importance. This is the focus of the present paper. For the reasons outlined above, attention will focus here on LONGUET-HIGGINS (1983) model that depends on a "measurable" spectral width parameter.

BACKGROUND

The joint distribution for wave heights and periods proposed by LONGUET-HIGGINS (1983) is

$$p(H', T') = \frac{2}{\nu\sqrt{\pi}} \frac{H'^2}{T'^2} L(\nu) \exp\left\{-H'^2\left[1 + \frac{(1 - 1/T')^2}{\nu^2}\right]\right\}$$

where

$$L(\nu) = \frac{2}{1 + (1/\sqrt{1 + \nu^2})}$$

and

$$H' = \frac{H}{2\sqrt{2\mu_0}} \qquad T' = \frac{T}{2\pi(\mu_0/\mu_1)}.$$

H' and T' are the normalized wave height and period, respectively; H and T are the respective dimensional wave height and period. This joint distribution is uniquely defined by the spectral width parameter ν, where

$$\nu = \sqrt{\frac{\mu_0\mu_2}{\mu_1^2} - 1}$$

and μ_0, μ_1, and μ_2 are moments of the variance density spectrum. The nth moment of the variance density spectrum is given by

$$\mu_n = \int_0^\infty f^n S(f)\, df$$

where f is a frequency and $S(f)$ is the corresponding variance density. The distribution is formally valid for $\nu^2 \ll 1$, which Longuet-Higgins assumes to hold for $\nu^2 < 0.36$.

DATA BASE

Data for this study were obtained from laboratory and field experiments. A summary of the characteristics of the laboratory and field data used herein is given in Table 1.

The laboratory experiments were conducted in the 103 m wind-wave flume at the Canada Centre for Inland Waters, Burlington. Random waves were generated from a DHH spectrum after DONELAN *et al.* (1985). Corrections were made to the piston-type wave board drive signal to correct for spurious, second-order long waves that arise through the mechanical generation of waves. Runs GR18-21 and GR22-25 were selected from the data set for analysis. Run GR18-21 is a fully-developed spectrum of waves with a peak period of 1.66 s, whereas run GR22-25 is a strongly forced spectrum with a peak period of 1.66 s also. These two runs were selected because they nicely illustrate the evolution of the joint distribution of wave heights and periods associated with wave shoaling while contrasting the differences between a fully-developed spectrum versus a strongly-forced spectrum. Each ensemble of laboratory runs yields approximately 2000 waves from which to construct the joint distribution of wave heights and periods. The runs were conducted on an impervious (plywood) beach with a slope of 1:20 (Figure 1). The 1:20 beach slope is similar to the 1:25 slope on which the field data was obtained. The cross-shore variation of wave heights and periods were determined from a synoptic set of ten surface-piercing capacitance-type wave probes. Analog outputs from the wave probes were low-pass filtered at 10 Hz then sampled digitally (with 12 bit resolution) at 20 Hz.

The field data were obtained at Queensland Beach, Nova Scotia. Queensland Beach is a nearly planar beach with a nearshore slope of approximately 1:25. It is exposed to the Atlantic Ocean by a relatively narrow "window" that significantly restricts the directional spread of the incident wave field (Figure 2). As a result, the incident wave field is essentially two-dimensional. Two records collected on the 25th and

→

Figure 3. (a) Short segment of the surface displacement time series from (top to bottom) wave probes 1, 7, & 9 on the 1:20 beach slope for runs GR18-21. The still water depths are 0.944, 0.357, and 0.161 m, respectively. Note the traces have been displaced for plotting purposes. (b) Spectra corresponding to the 3 surface displacement time series shown in panel a: solid, WP 1; dashed, WP 7; and dotted WP 9. There are 100 d.o.f. (c–e) Contours of joint distribution of wave heights and periods for WP 1 7, & 9, respectively. Dotted contours show theoretical expectation from Longuet-Higgins (1983). Contours are shown for (0.1, 0.3, 0.5, 0.7, 0.9, 0.99) × p_{max}.

Figure 4. (a) Short segment of the surface displacement time series from (top to bottom) wave probes 1, 7, & 9 on the 1:20 beach slope for runs GR22-25. The still water depths are 0.944, 0.357, and 0.161 m, respectively. Note the traces have been displaced for plotting purposes. (b) Spectra corresponding to the 3 surface displacement time series shown in panel a: solid, WP 1; dashed, WP 7; and dotted WP 9. There are 100 d.o.f. (c–e) Contours of joint distribution of wave heights and periods for WP 1 7, & 9, respectively. Dotted contours show theoretical expectation from Longuet-Higgins (1983). Contours are shown for (0.1, 0.3, 0.5, 0.7, 0.9, 0.99) × p_{max}.

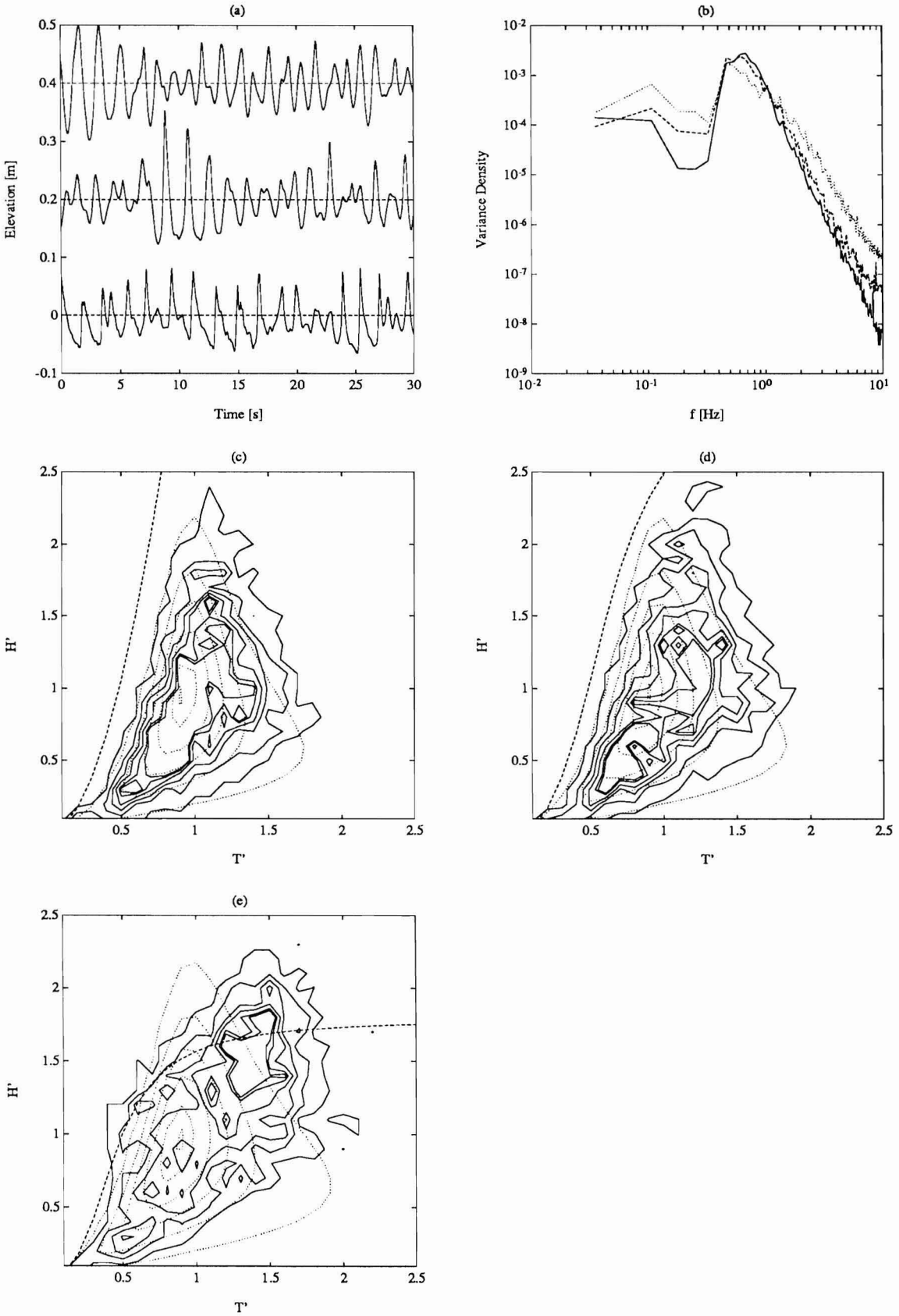
(a)
Elevation [m]
Time [s]
(b)
Variance Density
f [Hz]
(c)
H'
T'
(d)
H'
T'
(e)
H'
T'

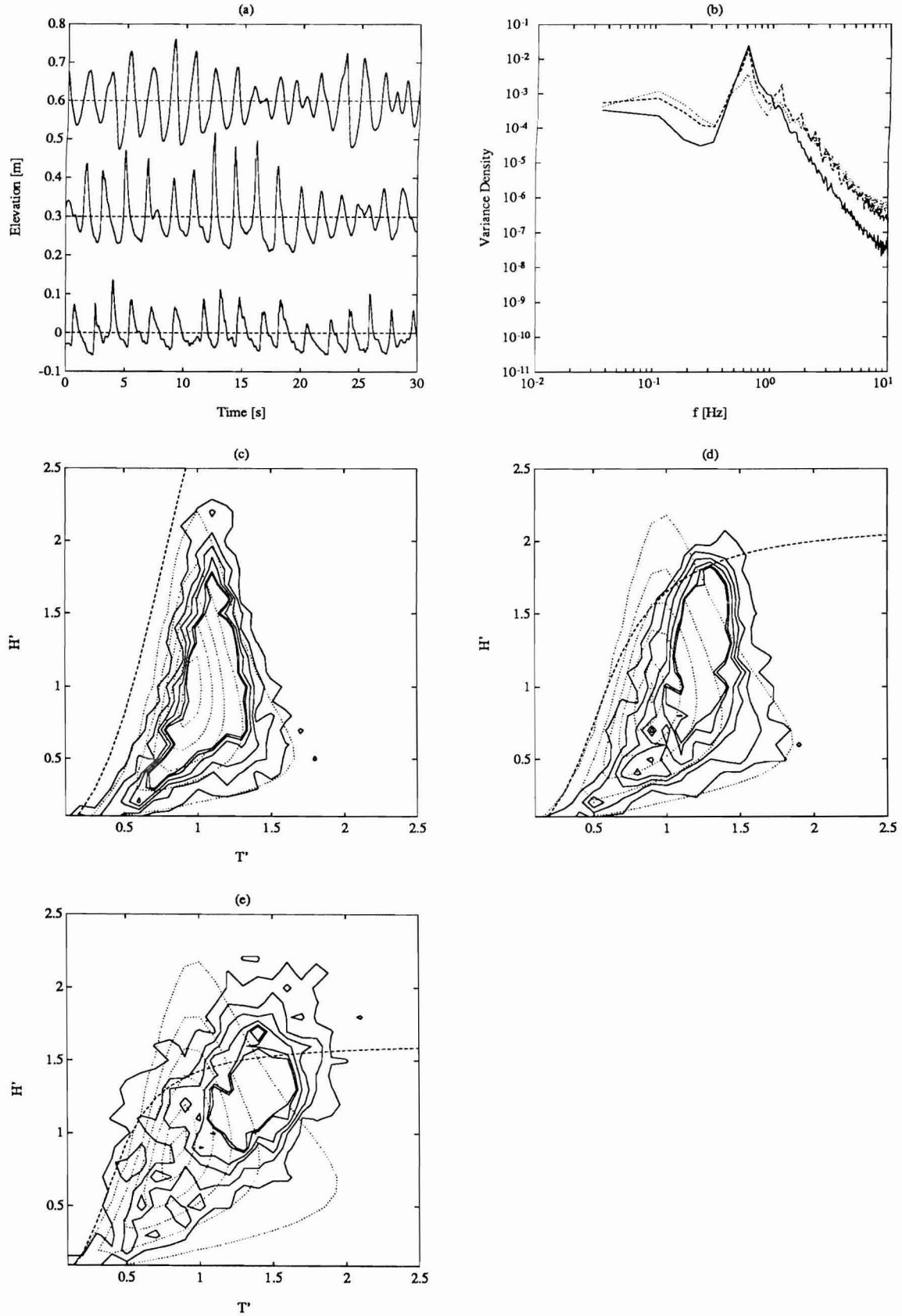
(a)
Elevation [m]
Time [s]
(b)
Variance Density
f [Hz]
(c)
H'
T'
(d)
H'
T'
(e)
H'
T'

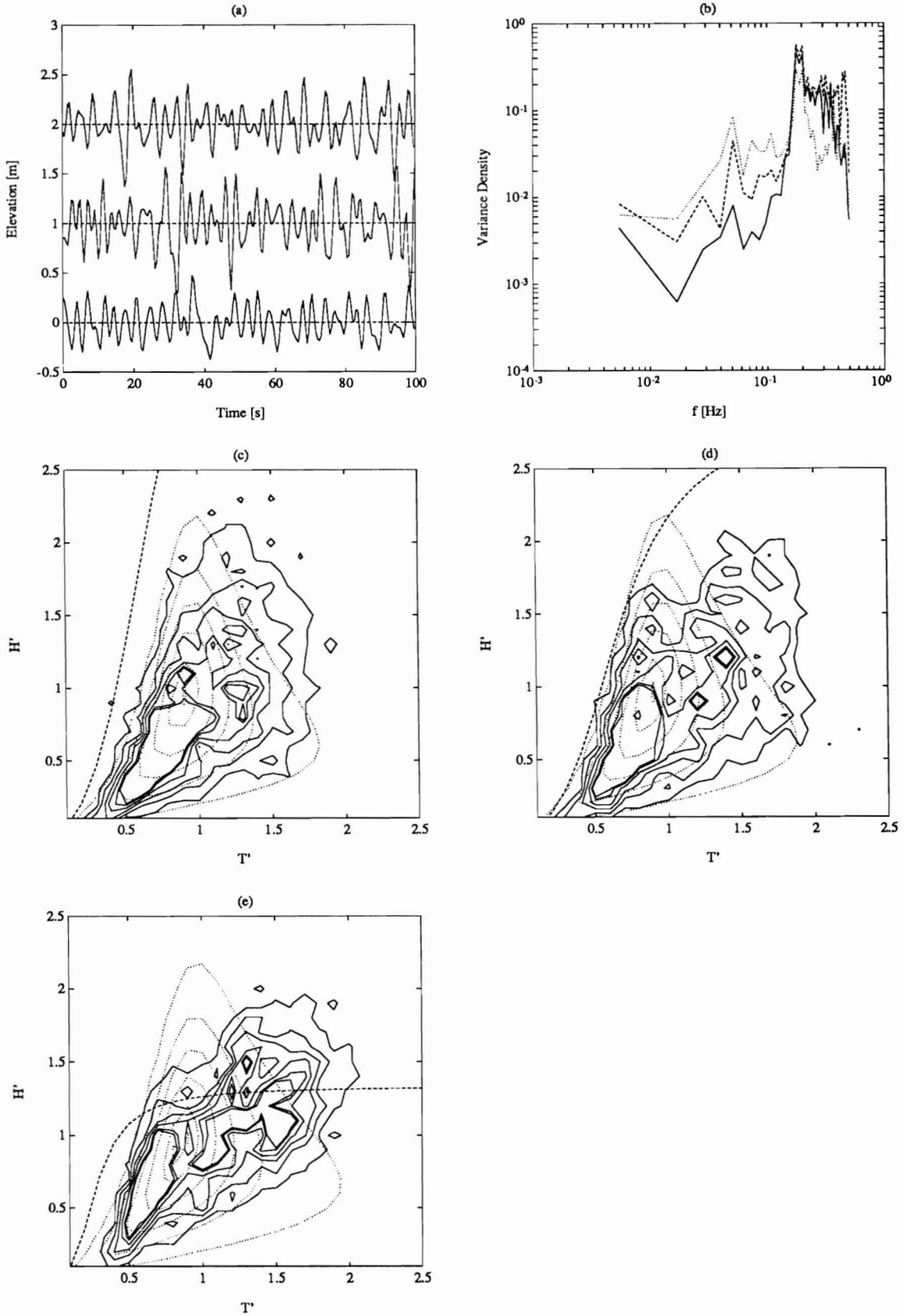
(a)
Elevation [m]
Time [s]
(b)
Variance Density
f [Hz]
(c)
H'
T'
(d)
H'
T'
(e)
H'
T'

29th of October 1987 were selected from the Queensland data set for analysis. Data from the 25th were chosen because this was the most energetic period observed, with inshore wave heights in excess of ≈ 1 m (this provides a comparison to strongly forced laboratory data), while data from the 29th were selected for their rather large amplitude swell. Wave heights and periods were determined from a cross-shore array of near-bottom mounted pressure sensors. Each ensemble of runs yields approximately 1500 waves from which to construct the joint distribution. Runs were selected around low/high tide to minimize nonstationary. Analog outputs from the pressure sensors were low-pass filtered at 1.0 Hz then sampled digitally (with 12 bit resolution) at 4 Hz.

DATA REDUCTION

The wave heights and periods for the laboratory and field data were determined using a zero-upcrossing analysis, as required for LONGUET-HIGGINS (1983) model. The procedure for computing the heights and periods for the laboratory data was as follows. The mean water level was removed and zero-upcrossings were identified. To eliminate the 20 Hz sampling quantization, the time of each zero-upcrossing was estimated using linear interpolation.

The procedure for computing the heights and periods for the field data was similar to that used for the laboratory data, with the following exceptions. The digital data were low-pass filtered at 0.5 Hz then decimated to 1 Hz. Linear theory was used to convert the near-bottom pressure record to sea surface displacement. The data were then quadratically detrended to remove any tidal signature. The wave heights and periods were determined from the resulting time series. A linear interpolation scheme was also employed for the field data to eliminate the 4 Hz sampling quantization that would occur in the wave period estimates.

OBSERVATIONS AND DISCUSSION

The model of LONGUET-HIGGINS (1983) was chosen here for comparison to the laboratory and field data because it is relatively insensitive to the high frequency cut off compared to other models. A more detailed description of the sensitivity of spectral moments to the high frequency cut off is given in DOERING and DONELAN (1993).

A short segment of the surface elevation from run GR18-21 on the 1:20 laboratory beach is shown Figure 3a. Note the records have been shifted for plotting purposes. The waves recorded at WP 1 (Figure 3a, top trace) are relatively symmetric with respect to the mean water level shown by the dashed line. However, in shallower depths of water (WP 7 and WP 9) there is a pronounced peaking of the wave crests and elongation of the troughs.

Figure 3b shows the spectra corresponding to the three surface displacement records shown in Figure 3a. The spectra from WP 1 and 7 are essentially coincident with the exception of the low frequency tail. The spectrum for WP 9, however, lies below those for WP 1 and 7 and has a smaller high frequency tail slope (*i.e.*, a relative increase in high frequency energy). The variation of the low frequency energy observed in Figure 3b is probably due to quasi-standing long waves that arise from radiation stress effects associated with wave groupiness. It is unlikely that this energy arises from the wave generation process as an effective second-order, long wave suppression algorithm was incorporated into the wave generation software.

Figures 3c to 3e show the evolution of the joint probability of wave heights and periods associated with shoaling. Recall that run GR18-21 is a fully-developed spectrum of waves with T_p = 1.67 s and H_s = 0.14 m. At the toe of the beach (WP 1), where ν = 0.30, there is good agreement between the observed and predicted distributions. Reasonable agreement is also observed at WP 7 where ν = 0.35. However, Figure 3e indicates that after breaking (ν = 0.42) the joint distribution is not well described. This is not particularly surprising as the breaking process significantly alters the joint distribution of wave heights and periods to a non-Gaussian form. Note, the most probable joint occurrence shifts to waves of larger heights and longer periods.

The dashed line shown in Figures 3c to 3e is the finite depth wave steepness limit given by MICHE (1944),

$$\left(\frac{H}{L}\right)_{\max} = 0.142 \tanh\left(\frac{2\pi d}{L}\right)$$

where d is the local water depth and L is the local wavelength. For the unbroken wave locations (*i.e.*, WP 1 and 7) the Miche limit defines the left-hand edge of both the theoretical and observed distributions. This is an intriguing observation, as LONGUET-HIGGINS (1983) joint distribution is a mathematical model for random noise and contains no wave physics. Figure 3e clearly indicates that the Miche limit does not apply for broken waves.

Figure 4 shows the results for run GR22-25, which is a strongly forced spectrum of waves with T_p = 1.67 s and H_s = 0.25 m shoaling on the 1:20 beach. The evolution of the waves is similar to that observed for run GR18-21. The waves at the toe of the beach (WP 1) are horizontally and vertically symmetric. However, shoaling produces very peaked wave crests and steep wave fronts. The strongly forced nature of these waves can be seen in the comparatively large wave heights (Figure 3a versus 4a). The spectra associated with these waves are shown in Figure 4b. The strongly forced nature of these waves is also reflected in the peakier spectra. Figures 4c to 4e show the observed and predicted joint distributions of wave heights and periods for run GR22-25. Inspection of Figure 4c indicates that the strongly forced nature

←

Figure 5. (a) Short segment of the depth corrected time series from (top to bottom) pressure sensors P2 (deepest), P4, & P6 (shallowest) at Queensland beach for runs QA25N5-P2. Note the traces have been displaced for plotting purposes. (b) Spectra corresponding to the 3 records shown in panel a: solid, P2; dashed, P4; and dotted P6. There are 40 d.o.f. (c–e) Contours of joint distribution of wave heights and periods for P2, P4, & P6, respectively. Dotted contours show theoretical expectation from Longuet-Higgins (1983). Contours are shown for (0.1, 0.3, 0.5, 0.7, 0.9, 0.99) × p_{max}.

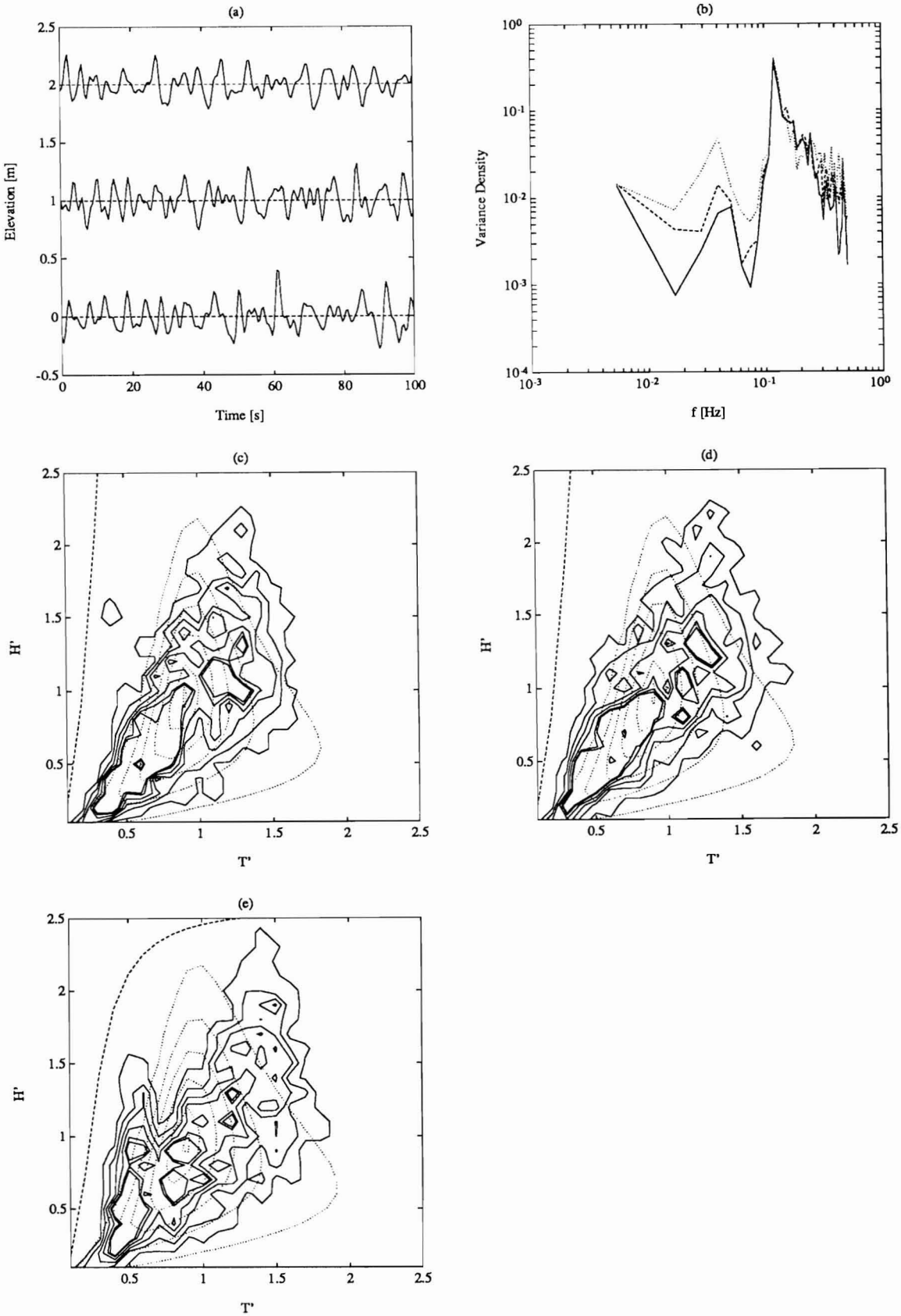
(a)
Elevation [m]
Time [s]
(b)
Variance Density
f [Hz]
(c)
H'
T'
(d)
H'
T'
(e)
H'
T'

of these waves is also evident in the relatively narrow joint distribution. The agreement between the observed and predicted distributions at WP 1 is reasonable ($\nu = 0.25$). However, the inception of wave breaking around WP 7 diminishes the agreement ($\nu = 0.37$). The agreement at WP 9, which is well inside the region of active breaking, is poor ($\nu = 0.42$). Figure 4e indicates there is a distinct shift of the most probable joint occurrence to larger wave heights with longer periods, similar to what was observed for the fully developed spectrum of waves (*i.e.*, run GR18-21). This shift in the most probable joint occurrence is also evident at WP 7.

The field data observations from Queensland Beach for runs QA25N5-P2 and QA29G4-I1 are shown in Figures 5 and 6, respectively. Recall the characteristics of these two runs are quite different. Run QA25N5-P2 was the most energetic period during this field experiment with a peak period of 6.3 s and inshore wave heights in excess of 1 m (see Figure 5a). Run QA29G4-I1 was a relatively calm period with a well defined, relatively large amplitude ($H_c = 0.40$ m) incident swell ($T_p = 8.0$ s).

Figure 5a shows a sample of the depth corrected, surface displacement time series from pressure sensors P2, P4, and P6, which were located in water depths of 4.29, 3.19, and 0.97 m, respectively. Note, the relatively large wave observed at t $\approx$ 20 s in the P2 record can be readily identified in both the P4 and P6 records. Figure 5b shows the spectra corresponding to the sea surface displacement records shown in figure 5a. Of interest is the dramatic redistribution of energy from P2 to P4, and from P4 to P6. In particular, there is a significant increase in both harmonic and low frequency (subharmonic) energy from P2 to P4, whereas from P4 to P6 there is a considerable loss of harmonic energy (less than initial observed at P2) and further enhancement of low frequency energy from P4 to P6. Figures 5c to 5e show the evolution of the joint distribution of wave heights and periods for run QA25N5-P2. The agreement at the deepest station (P2) where $\nu = 0.34$ is reasonable. However, breaking further inshore leads to poor agreement at P4 and P6, where ν equals 0.38 and 0.43, respectively. The Miche limit (shown by the dashed line) seems applicable at P2, is questionable at P4, and is obviously not applicable at P6 as a result of wave breaking. In contrast to the observations of the laboratory data, there is no clear tendency for the most probable joint occurrence to shift towards larger wave heights and periods as the waves shoal and break.

A short segment of the depth corrected surface displacement records, corresponding spectra and joint distributions for run QA29G4-I1 are shown in Figures 6a to 6e. The spectra indicates the relatively narrow banded characteristic of this run. As for run QA25N5-P2 there is an (apparent) increase in the low frequency energy arising from shoaling. The joint distribution of wave heights and periods is not well predicted at any of the three stations. The lack of agreement is likely due to the relatively shallow water nature of these waves, *i.e.*, $\nu > 0.35$ for all 3 stations.

SUMMARY

The evolution of the joint distribution of wave heights and periods associated with wave shoaling was investigated using laboratory and field data. The laboratory data were collected on a 1:20 planar beach slope, whereas the field data were obtained on a nearly planar beach with a nearshore slope of 1:25. The data were compared to the joint distribution of wave heights and periods proposed by LONGUET-HIGGINS (1983).

The comparison between the data and LONGUET-HIGGINS (1983) joint distribution indicates that LONGUET-HIGGINS (1983) distribution provides a reasonable fit to both the laboratory and field data if the waves are unbroken and $\nu < 0.35$, which is somewhat less than the value of 0.6 for which LONGUET-HIGGINS assumes his joint distribution is applicable. The suggestion is LONGUET-HIGGINS (1983) is not suitable for spectral widths greater than about 0.35. The Miche limit for finite depth wave steepness nicely envelopes unbroken waves for both the laboratory and field data, but does not describe broken wave data.

It was noted that the observed and predicted distributions (for both the laboratory and field data) are not coincident, but are shifted slightly in both height and period. The most probably observed height and period for unbroken laboratory data are slightly larger than predicted. However, the opposite was observed for unbroken field data, *i.e.*, the most probable observed height and period are slightly smaller than predicted.

ACKNOWLEDGEMENTS

The laboratory research was conducted while the author was a Visiting Fellow with Dr. M.A. Donelan at the National Water Research Institute, Canada Centre for Inland Waters, Burlington. The laboratory research was funded by the Panel for Energy Research and Development (PERD), and was lead by Dr. M.G. Skafel. The field data was obtained from the C-COAST project, which was funded by an NSERC strategic grant to Drs. B. Greenwood & A.J. Bowen. The analysis and synthesis of the data was supported by the author's NSERC research grant.

LITERATURE CITED

CARTWRIGHT, D.E. and LONGUET-HIGGINS M.S., 1956. The statistical distribution of the maxima of a random function. *Proceedings Royal Society London*, Ser. A., 237, 212–232.

CAVANIE, A.; ARHAN, M., and EZRATY, R., 1976. A statistical relationship between individual heights and periods of storm waves. *Proceedings B.O.S.S.*, 354–360.

←

Figure 6. (a) Short segment of the depth corrected time series from (top to bottom) pressure sensors P2 (deepest), P4, & P6 (shallowest) at Queensland beach for runs QA29G4-I1. Note the traces have been displaced for plotting purposes. (b) Spectra corresponding to the 3 records shown in panel a: solid, P2; dashed, P4; and dotted P6. There are 40 d.o.f. (c–e) Contours of joint distribution of wave heights and periods for P2, P4, & P6, respectively. Dotted contours show theoretical expectation from Longuet-Higgins (1983). Contours are shown for (0.1, 0.3, 0.5, 0.7, 0.9, 0.99) $\times$ p_{max}.

DOERING, J.C. and DONELAN, M.A., 1993. The joint distribution of heights and periods of shoaling waves. *Journal Geophysical, Research*, 98(C7), 12,543–12,555.

DONELAN, M.A.; HAMILTON, J., and HUI, W.H., 1985. Directional spectra of wind-generated waves. *Philosophical Transactions, Royal Society London, Series A.*, 315, 509–562.

GODA, Y., 1978. The observed joint distribution of periods and heights of sea waves. *Proceedings International Conference Coastal Engineering*, 16th, 227–246.

LINDGREN, G. and RYCHLIK, I., 1982. Wave characteristic distributions for Gaussian waves—Wave-length, amplitude, and steepness. *Ocean Engineering*, 9, 411–432.

LONGUET-HIGGINS, M.S., 1957. The statistical analysis of a random, moving surface. *Philosophical Transactions Royal Society London, Series. A*, 249, 321–387.

LONGUET-HIGGINS, M.S., 1975. On the joint distribution of the periods and amplitudes of sea waves. *Journal Geophysical Research*, 80(18), 2688–2694.

LONGUET-HIGGINS, M.S., 1983. On the joint distribution of wave periods and amplitudes in a random wave field. *Proceedings Royal Society London Series A.*, 389, 241–258.

MICHE, R., 1944. Mouvements ondulatoires de la mer en profondeur constante ou decroissante. *Ann. Ponts Chaussees.*

OSBORNE, P.D. and GREENWOOD, B., 1992. Frequency dependent cross-shore suspended sediment transport. 1. A non-barred shoreface. *Marine Geology*, 106, 1–24.

RICE, S.O., 1944. The mathematical analysis of random noise. *Bell System Technical Journal*, 23, 282–332.

RICE, S.O., 1945. The mathematical analysis of random noise. *Bell System Technical Journal*, 24, 46–156.

SROKOSZ, M.A. and CHALLENOR, P.G., 1987. Joint distributions of wave height and period: a critical comparison. *Ocean Engineering*, 14(4), 295–311.

WOODING, R.A., 1955. An approximate joint probability distribution for amplitude and frequency in random noise. *New Zealand Journal Science Technology*, B36, 537–544.

YUAN, Y., 1982. On the statistical properties of sea waves. Ph.D. Thesis, North Carolina State University, 80p.